

$$= -\alpha T v \left( \frac{dM}{dT} \right) \left( \frac{dH}{d\epsilon} \right) / c_p \quad \text{for } x = \frac{d\epsilon}{dH}.$$

$\alpha$  is the linear thermal-expansion coefficient,  $c_p$  is the specific heat per mole, and  $v$  is the molar volume ( $\approx 57 \text{ cm}^3$  for  $\text{Sc}_3\text{In}$ ).

<sup>9</sup>W. P. Mason, Phys. Rev. **83**, 683 (1951); see also L. R. Testardi and J. H. Condon, Phys. Rev. B **1**, 3928 (1970).

<sup>10</sup>This behavior and the observed isotropy with respect to field and propagation directions are also consistent with the superparamagnetic state (but see Ref. 6).

<sup>11</sup>Specific-heat data for  $\text{Sc}_3\text{In}$  below 4 °K have recently

been reported by L. L. Issacs and G. S. Knapp, Bull. Am. Phys. Soc. **15**, 1623 (1970). More detailed data are given by L. L. Isaacs, G. S. Knapp, and H. V. Culbert (unpublished).

<sup>12</sup>This is the Curie temperature reported by Gardner *et al.* (Ref. 2) and defined as the temperature where a spontaneous moment (obtained by extrapolation from  $H > 1 \text{ kOe}$ ) should occur. A value of 6.1 °K was obtained by these authors using initial susceptibility data.

<sup>13</sup>This approximation is usually good to better than 10%. It fails in the rare case of large selective acoustic mode softening and damping.

## Magnetothermal Properties of Heat Transport in Cobalt Chloride Thiourea\*

C. Ni,<sup>†</sup> H. N. Spector, and H. Weinstock

*Department of Physics, Illinois Institute of Technology, Chicago, Illinois 60616*

(Received 24 January 1972)

Thermal-conductivity measurements have been made on a single crystal of cobalt chloride thiourea,  $\text{CoCl}_2 \cdot [(\text{NH}_2)_2\text{CS}]_4$ , in the temperature range 0.35–20 K and in applied magnetic fields of up to 20 kG. Below the Néel temperature of 0.92 K, an enhancement in conductivity for heat flowing in the [001] sublattice-magnetization direction is interpreted as due to the onset of spin-wave conductivity. Data taken for heat flowing in a normal [110] direction show no such enhancement. Relatively sharp changes in the conductivity as a function of temperature and magnetic field have been used to obtain information on the paramagnetic-antiferromagnetic and antiferromagnetic-spin-flop phase boundaries. Magneto-thermal-resistance resonances in the paramagnetic state have yielded information on the magnitude and anisotropy of the  $g$  value for the unpaired electronic state of the cobalt ion.

### I. INTRODUCTION

At low temperatures, the statistical properties of a physical system are determined by the low-lying excitations of the system. Spin-wave theory has been recognized as providing a successful model for studying magnetic substances in this regime. In an antiferromagnet, the magnetic ions are (super)exchange coupled to their neighbors in such a way that the long-range ordering which occurs below the Néel temperature ( $T_N$ ) leads to a spontaneous magnetization. Antiferromagnetic spin waves are generated from an ordered array of alternately pointing spins, which on the basis of Anderson's calculation<sup>1</sup> for the antiparallel-spin-sublattice model is a reasonable approximation of its ground state. Experimental evidence for the excitation of antiferromagnetic spin waves of definite wave vector has been observed in antiferromagnetic resonance measurements for  $q = 0$  by Jacobs *et al.*<sup>2</sup> and others,<sup>3,4</sup> and from neutron-inelastic-scattering measurements for  $q \neq 0$  by Okazaki *et al.*<sup>5</sup> Such collective excitations could transport energy at low temperatures provided  $T < T_N$ . It was first speculated by Sato<sup>6</sup> that it may be of interest to measure the thermal conductivity of an antiferromagnet. Since then, antiferromagnetic-spin-wave

heat-transport observations were attempted in a variety of antiferromagnetic insulators by Slack,<sup>7</sup> by Donaldson and Edmonds,<sup>8</sup> and by Gorter and Tinbergen.<sup>9</sup> However, positive identification of spin-wave thermal-energy transport has not been made in the investigated insulating systems.

A preliminary report by Weinstock<sup>10</sup> (on two crystals other than those used in the current study) indicated that there might be a possible antiferromagnetic-spin-wave contribution to the thermal conductivity of antiferromagnetic cobalt chloride thiourea. Some useful physical properties of this crystal are summarized in the Appendix.

This particular crystal system appears to be a good one for attempting to identify antiferromagnetic-spin-wave heat transport. It is a uniaxial two-sublattice system, with its spontaneous-magnetization direction along the [001] direction. For such a relatively simple magnetic structure, theoretical analysis is available.

Another important feature is that the Néel temperature is much lower than the Debye temperature, i. e.,  $T_N \ll \Theta_D$ . The Néel temperature has been determined by both heat-capacity<sup>11</sup> and susceptibility<sup>12</sup> measurements to be 0.92 K, while the same heat-capacity work carried to higher temperature yields  $\Theta_D \approx 65 \text{ K}$ . These heat-capacity

data are also useful in that they show a  $T^3$  temperature dependence at temperatures above  $T_N$ . This implies that a Debye spectrum of phonons may be assumed in analyzing the thermal conductivity below  $T_N$ .

Although the above-stated condition ( $T_N \ll \Theta_D$ ) implies it is possible for spin-wave conduction to dominate a phonon-conduction term below  $T_N$ , it remains to be seen whether an appreciable number of spin waves can be excited in the temperature region from the lowest temperature attainable (0.35 K) to  $T_N = 0.92$  K. Using a two-sublattice model for a body-centered-tetragonal system, the magnon-dispersion relation in the spontaneous  $c$  direction of magnetization is given (either semi-classically or quantum mechanically) by<sup>13,14</sup>

$$h\omega_{\vec{q}}^{\pm} = g\mu_B [(H_E + H_A)^2 - H_E^2(1 - 2q^2 c^2/z)]^{1/2} \pm g\mu_B H \quad (1)$$

in the limit  $qc \ll 1$ , where  $\omega_{\vec{q}}$  is the normal mode frequency of the antiferromagnetic wave vector  $\vec{q}$  in the  $c$  direction,  $H_E$  is the effective exchange field,  $H_A$  is the effective anisotropy field,  $H$  is the applied field,  $c$  is the lattice constant in the  $c$  direction, and  $z$  is the coordination number. Spin waves described by this relation are doubly degenerate, and due to the anisotropy-exchange coupling, there exists a gap in the spin-wave spectrum at  $\vec{q} = 0$  (and  $H = 0$ ) called the anisotropy-exchange gap. Corresponding to this gap, a temperature  $T_{AE}$  is defined such that<sup>15</sup>

$$T_{AE} = (g\mu_B/k_B)(2H_A H_E + H_A^2)^{1/2}. \quad (2)$$

Below  $T_{AE}$ , the number of excited spin waves falls off exponentially to zero. Application of a magnetic field removes the degeneracy in the spectrum, driving one branch to higher frequencies, the other to lower frequencies. At some critical field ( $H_C$ ), the lower branch reaches a value of  $\omega_{\vec{q}} = 0$  for  $\vec{q} = 0$ , and the system undergoes a transition into the less correlated spin-flop state. It has been found<sup>16</sup> that the critical spin-flop field can be expressed as

$$H_C^2 = \frac{2H_A H_E + H_A^2}{1 - \chi_{\parallel}/\chi_{\perp}}, \quad (3)$$

where  $\chi_{\parallel}$  and  $\chi_{\perp}$  are the parallel and perpendicular susceptibilities relative to the  $c$  direction of sublattice magnetization. Combining Eqs. (2) and (3), it is found that

$$T_{AE} = (g\mu_B H_C/k_B)(1 - \chi_{\parallel}/\chi_{\perp})^{1/2}. \quad (4)$$

Using published susceptibility data<sup>12</sup> and a result obtained for  $H_C$  in the currently reported study, it is found that  $T_{AE} \approx 0.5$  K.<sup>17</sup> Thus, due primarily to the relatively small anisotropy field, it appears that spin waves should be excitable in the temperature range being investigated.

Finally, since this system is one for which the Néel temperature is much smaller than the (temperature-equivalent) separation of doublets, the mixing of doublets due to exchange interaction can be neglected, and only the lowest-lying doublet needs to be considered. Under this assumption there are only two spin states per cobalt ion. Thus, all spin operators can be expressed in terms of a fictitious spin of  $\frac{1}{2}$ . Evaluating the entropy change (from specific-heat data) on going through the paramagnetic-antiferromagnetic phase transition shows this to be a reasonable assumption; i. e., a value of  $\Delta S = R \ln 2/\text{mole}$  was found.

## II. EXPERIMENTAL DETAILS

The steady-state method was used to measure thermal conductivity. Because of the low Néel temperature, a  $^3\text{He}$  refrigeration system was used covering the temperature range 0.35–1.2 K. Two Ohmite  $\frac{1}{8}$ -W 5% tolerance carbon-composition resistors, each of 12- $\Omega$  nominal value, were chosen as matched thermometers in the above-mentioned temperature range to measure the temperatures at two points along the specimens after a steady-state temperature gradient was established by feeding power into the crystal heater—see Fig. 1. The basic refrigeration, measuring circuitry, vacuum systems, and the technique of operation are described elsewhere.<sup>18</sup> Only the special features of the cryostat, shown in Fig. 1, pertaining to the particular experimental design will be described.

### A. Crystal Holder

In order to place the crystal in the center segment of a fixed-position superconducting solenoid without significantly reducing the linkage to the  $^3\text{He}$  cryostat, a large-cross-section copper bar was used. The top end of the bar is disk shaped, 1 in. in diameter and  $\frac{1}{8}$  in. in thickness, with screw threads extending upward (from the center of the disk) which are threaded into the base on the liquid- $^3\text{He}$  reservoir. The matching surfaces of the  $^3\text{He}$  reservoir and the disk are highly flat and polished. On these surfaces, a thin film of Dow Corning 705 fluid was applied during assembly to ensure a good thermal contact. The lower end of the bar is an adapter for the crystal holder which can be mounted onto the bar at various angles with respect to the vertical axis. The length of the crystal holder is designed such that the two thermometers on the particular sample under investigation are located at the center of the superconducting magnet coils (where the field intensity is a maximum and has the greatest uniformity). This feature is essential for studying the magnetic anisotropy of a crystal specimen.

### B. Superconducting Magnet

A superconducting magnet with a maximum field intensity of over 22 kG was used. The magnet was supported by a brass flange. The mounting of the magnet is vertically adjustable to a small extent. Fourteen-gauge copper wire was recommended by the manufacturer for providing the coil current, but this thick highly (thermal-) conducting wire introduces a large heat leak into the liquid- $^4\text{He}$  bath. As a result, the bath temperature fluctuates in the presence of these wires. This difficulty was eliminated by installing inside the Dewar an electrical connector which can be totally removed when the magnet is in a persistent mode of operation.

### C. Crystal Preparation

Thermal-conductivity measurements were reproducible to within experimental error provided that the sample mounting was not disturbed. For this reason, a separate crystal holder was used for mounting each sample.

Single-crystal cobalt chloride thiourea was grown by evaporation at a constant temperature of  $20^\circ\text{C}$  from an aqueous solution containing cobaltous chloride  $\text{CoCl}_2 \cdot 6\text{H}_2\text{O}$  and thiourea  $(\text{NH}_2)_2\text{CS}$ . Due to the solubility difference between these two components at a given temperature, the simple use of relative amounts in proportion to the molecular weights of the constituents is not suitable for the

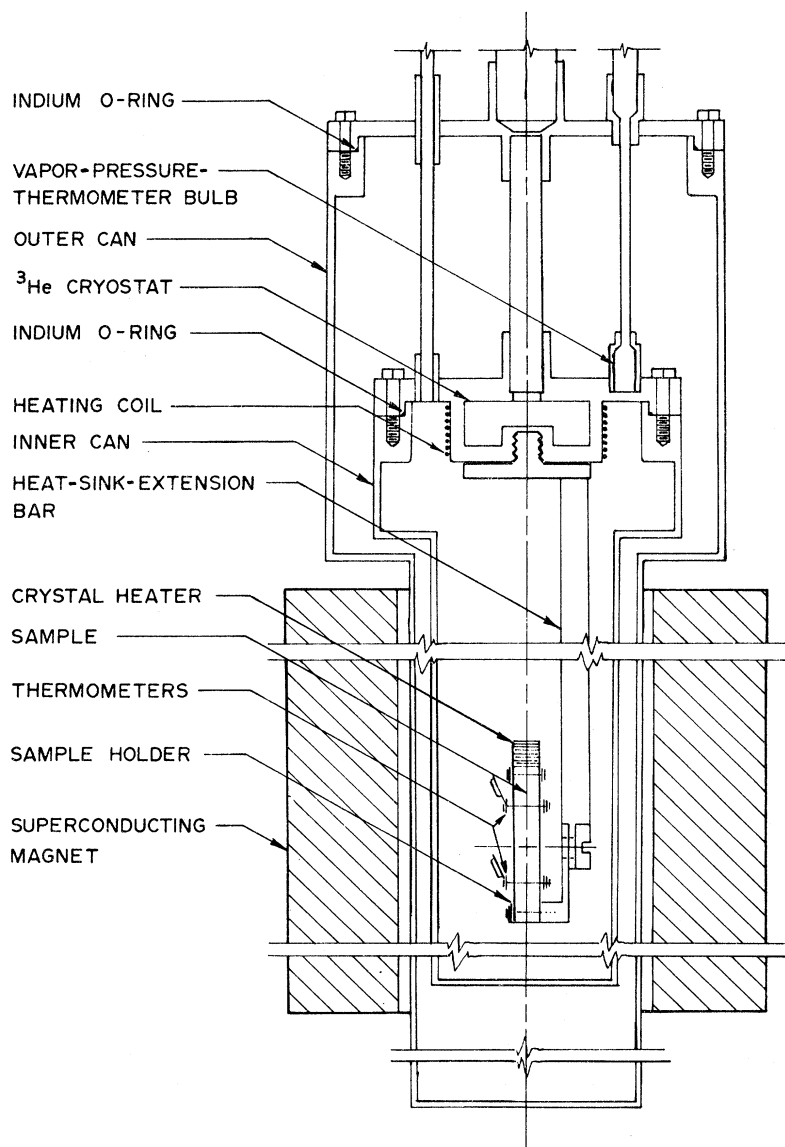


FIG. 1. Schematic of  $^3\text{He}$  cryostat for thermal-conductivity measurements with heat flow in arbitrary direction to magnetic field.

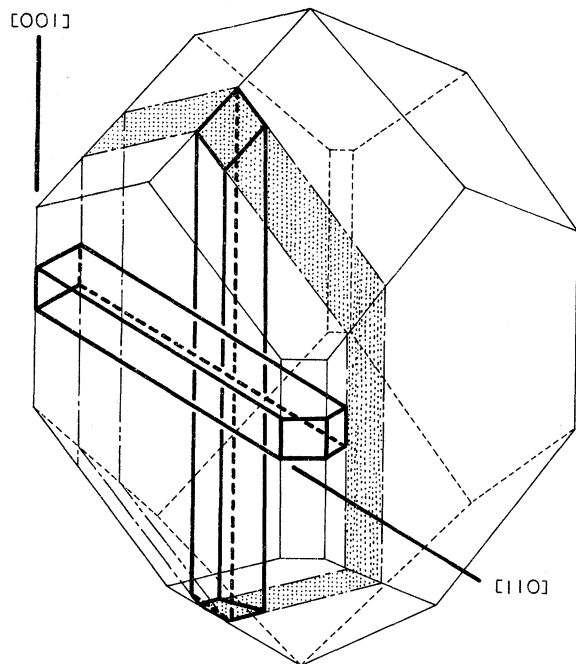


FIG. 2. Illustration of crystallographic orientation of samples 1 and 2 related to the geometry of a large single crystal (from which both were cut).

purpose of making a supersaturated solution. The proportion 2:1 by weight,  $\text{CoCl}_2 \cdot 6\text{H}_2\text{O} : (\text{NH}_2)_2\text{CS}$ , seems to work well at  $20^\circ\text{C}$ .

According to the facts presented in the Appendix, this species of crystal is both magnetically and crystallographically anisotropic. For the convenience of experimental data analysis, the samples for measurement were cut side by side from the same relatively large single crystal—see Fig. 2. These hereafter will be designated as samples 1 and 2. Sample 1 has its long axis parallel to the [001] direction, and sample 2 has its long axis perpendicular to the [001] direction and parallel to the [110] direction. Since the crystal has essentially uniaxial structure, the [110] and  $[\bar{1}\bar{1}0]$  directions will reveal the same information. The wet-string method was used to cut the original large single crystal, and the resultant samples were sanded down using crocus cloth to the rectangular shapes desired. A final light cleaning and etching of the surface was done on an S. S. White Industrial abrasive unit model No. F with No. 2-size abrasive powder (of calcium magnesium carbonate) to reduce the possibility of specular reflection of phonons and magnons. The final samples have the following sizes: sample 1:  $0.93 \times 0.16 \times 0.13$  in.; sample 2:  $0.87 \times 0.15 \times 0.14$  in. A few small pits were observed visually on the surfaces of the samples, but none were seen between the thermometers. The specimen crystals were mounted with

a desired orientation onto their crystal holders by means of phosphor-bronze clamps.

### III. RESULTS

The experimental results are best illustrated graphically in Figs. 3–9.

Figures 3 and 4 show the thermal conductivity of sample 1 as a function of temperature at constant applied-magnetic-field intensity; namely, at zero field and 10 kG. The magnetic fields were applied parallel or perpendicular to the [001] direction of the specimen in these measurements. The same procedures were carried out on sample 2 with the results presented in Figs. 5 and 6. The temperature dependence of the thermal conductivities shows anisotropic behavior throughout the entire temperature range measured, at zero magnetic field, as well as with fields applied parallel and perpendicular to the direction of heat flow. In every case, the thermal-conductivity curve at an applied field of 10 kG shows a unique  $T^3$  temperature dependence below  $T = 1.2$  K. Among the zero applied magnetic field curves, there is a depression in the vicinity of the paramagnetic-antiferromagnetic phase-transition temperature ( $T_N$ ). Below this transition temperature, sample 1 shows an enhancement in thermal conductivity at zero applied field, but no such enhancement occurs for

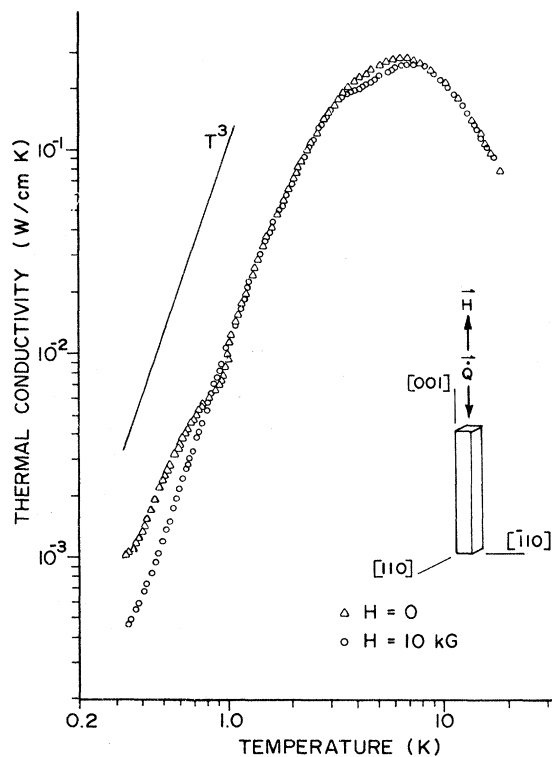


FIG. 3. Thermal conductivity vs temperature for magnetic field and heat flow in the [001] direction.

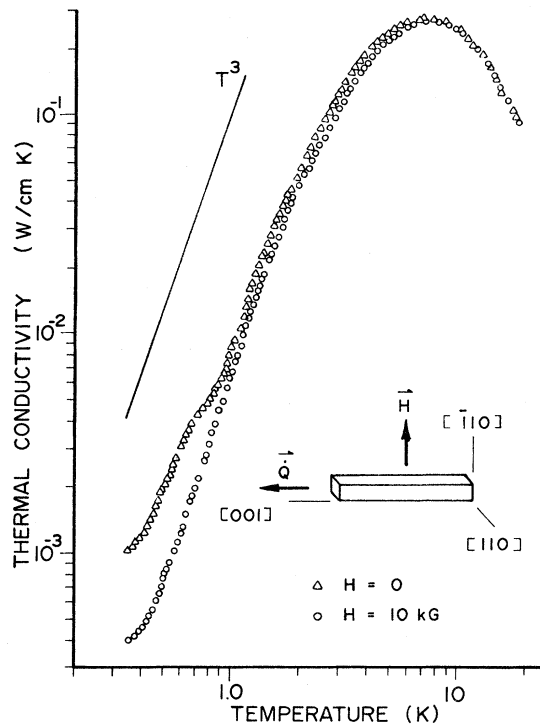


FIG. 4. Thermal conductivity vs temperature for magnetic field in the  $[110]$  direction and heat flow in the  $[001]$  direction.

sample 2.

Upon application of a magnetic field of  $H = 10$  kG to sample 1, the thermal conductivity is reduced by roughly 50% of its value in zero field at a temperature of 0.45 K. At higher applied-field intensities, this reduction is less, as shown in Fig. 7. This "recovery" of thermal conductivity with higher applied fields is better illustrated in Fig. 8 in which the ordinate axis is plotted in dimensionless form, using the ratio of thermal conductivity in the applied field ( $K_H$ ) to the thermal conductivity at zero field ( $K_0$ ). This ratio is plotted against the applied magnetic field intensity  $H$ . The resulting curve shows that the thermal conductivity (at 0.45 K) in the applied field initially decreases as the field intensity increases. The curve reaches a minimum  $K_H/K_0$  value (of about half of its zero-applied-field value) at  $H = 10$  kG, while  $K_H/K_0 \approx 0.75$  at  $H = 20$  kG. Numerical values used in Fig. 8 were obtained from thermal-conductivity measurements with various field intensities, namely,  $H = 0, 2, 4, 6, 8, 10,$  and  $20$  kG by interpolation at  $T = 0.45$  K from constant field curves of  $K_H$  vs  $T$ . At 0.45 K and below, it appears that one is sufficiently far from the phase-transition region in relatively low applied fields to be free of thermal effects due to critical fluctuations.

Figure 9 shows the data below  $T_N (= 0.92$  K) of

Fig. 3 on an expanded scale. The solid line in this figure represents the thermal conductivity due to phonon conduction derived from a functional fit of the zero-field conductivity assuming two components of heat transport, with crystal boundary scattering assumed to be the dominant scattering mechanism for the phonon component. The functional form chosen is  $K_0 = AT^\eta + BT^3$ . Analysis of the data using this form below 0.6 K yields

$$\eta = 1.8,$$

$$A = (3.9 \pm 0.1) \times 10^{-3} \text{ W/cm K}^{2.8},$$

$$B = (1.0 \pm 0.1) \times 10^{-2} \text{ W/cm K}^4.$$

The solid line shown in Fig. 9 is a plot of the phonon component ( $K_{ph}$ ) of the total conductivity at zero applied field:

$$K_{ph} = BT^3 = 1.0 \times 10^{-2} T^3 \text{ W/cm K}.$$

This line coincidentally appears to be a best fit to the data obtained with a 10-kG applied field along the direction of sublattice magnetization.

The difference in thermal conductivity  $\Delta K = K_0 - K_{10}$  between the zero and 10-kG applied-field data points shown in Fig. 9, is also plotted as a function of temperature in Fig. 9. As expected from the foregoing analysis, this shows that above 0.6 K,  $\Delta K$  drops rapidly as temperature increases, and below 0.6 K,  $\Delta K$  has a  $T^{1.8}$  temperature de-

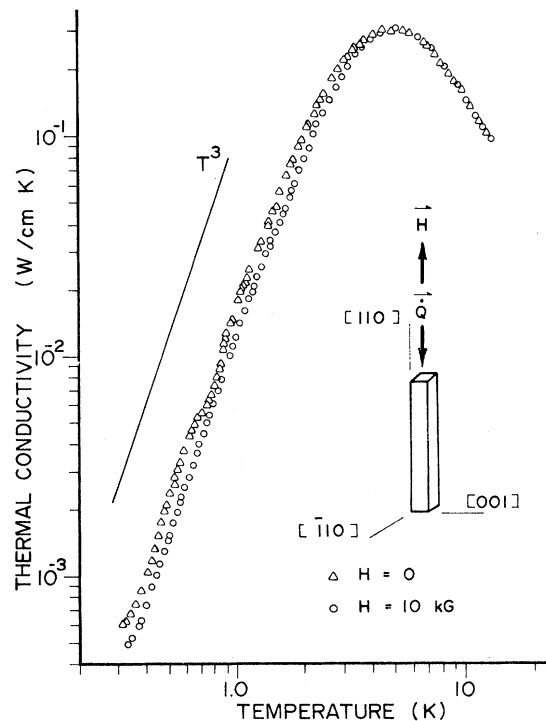


FIG. 5. Thermal conductivity vs temperature for magnetic field and heat flow in the  $[110]$  direction.

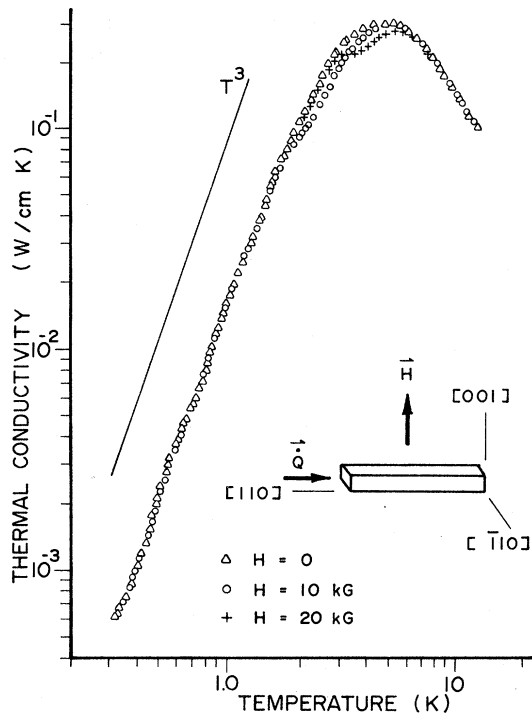


FIG. 6. Thermal conductivity vs temperature for magnetic field in the [001] direction and heat flow in the [110] direction.

pendence. Similarly with the data of Fig. 7 for 10- and 20-kG applied-field thermal conductivities of sample 1, defining  $\Delta K \equiv K_{20} - K_{10}$ , it is found that  $\Delta K$  has a  $T^{2.0}$  temperature dependence. Of some note is the fact that representing the 20-kG thermal-conductivity data by  $K_{20} = AT^n + BT^3$  yields the same value of  $B$  as does the similar analysis above for  $K_0$ .

To establish the validity of the experimental procedure used and to check for possible thermal hysteresis on going through the Néel temperature, experimental points were obtained on cooling and then on warming. No evidence of hysteresis was found to within the experimental precision of 2%.

The appearance of a small upturn in conductivity for  $T < 0.4$  K should be discounted, as this is due to instrumental limitations and appears for measurements done on a variety of crystal species.

#### IV. DISCUSSION

##### A. Theoretical Aspects of Magnon Conduction

In these experiments, an attempt has been made to determine the presence of the contribution of the antiferromagnetic magnons to the thermal conductivity. The experimental evidence, which has been presented in the Sec. III, indicates that below the Néel temperature there is an enhancement of

the thermal conductivity which can be explained in a reasonable fashion by the onset of magnon conduction.

A theory which explains, at least qualitatively, the essential features of a simple uniaxial antiferromagnetic material at low temperatures is the spin-wave approximation.<sup>15,19</sup> In this approximation, the coupled equations of motion of the spins on the two sublattices are linearized to lowest order in the spin-deviation operator  $n = a^\dagger a$ . Here  $a^\dagger$  and  $a$  are the creation and annihilation operators for a spin deviation from the sublattice magnetization direction, and  $\langle n \rangle$  determines the average number of spin deviations at a given temperature, i. e., the number of magnons thermally excited. The equations of motion are then solved to yield a dispersion relation for the antiferromagnetic magnons. The dispersion relation can then be used, together with the fact that magnons are Bose-Einstein quasiparticles, to determine the thermal and transport properties of the magnons, e. g., their contribution to the specific heat and the thermal conductivity.

The validity of the spin-wave approximation depends upon whether the linearization procedure is justified. Therefore, it is only quantitatively valid when the average spin deviation is much smaller

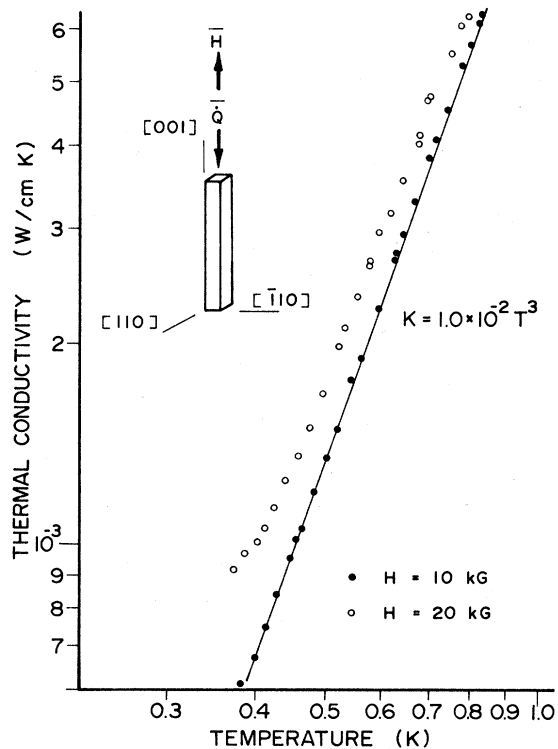


FIG. 7. Thermal conductivity vs temperature on an expanded scale (for  $T < T_N$ ) with magnetic fields of 10 and 20 kG and heat flow in the [001] direction.

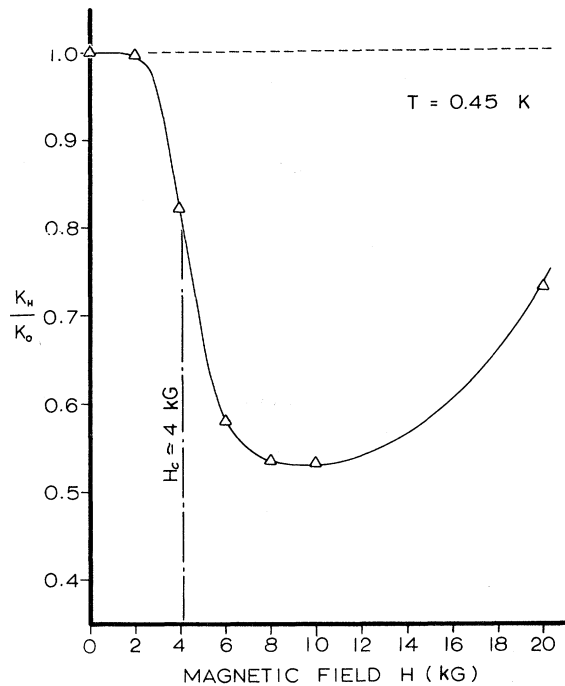


FIG. 8. Ratio of thermal conductivity in magnetic field  $H$  to that in zero field vs  $H$  at  $T=0.45$  K.

than the spin of the system. One would thus expect the spin-wave approximation to be valid at low temperatures where only a few magnons are excited. On the other hand, one would not expect the spin-wave theory to be valid in the vicinity of the Néel temperature ( $T_N$ ), where the number of magnons is large and nonlinear terms involving magnon-magnon interaction definitely cannot be neglected. One would expect that the spin-wave approximation would be valid only when  $T \ll T_N$ .

Unfortunately, in these experiments, the lowest temperatures attained (about 0.35 K) were not far enough below the Néel temperature of 0.92 K for the spin-wave theory to be applied unambiguously to the results. This also can be seen from the specific-heat measurements in the same material, which showed a  $T^{4.8}$  temperature dependence below the Néel temperature instead of the  $T^3$  dependence which would be expected from spin-wave theory. However, although one cannot apply spin-wave theory to interpret the results quantitatively, it can be used to give a qualitative discussion.

In the experiments it is found that there is an enhancement of the thermal conductivity at temperatures below the Néel temperature. This enhancement is attributed to magnon conductivity. The magnitude of the presumed magnon conductivity ( $K_m$ ) has been determined by analyzing the total conductivity in the form  $K = K_m + K_{ph}$ . From this analysis, it is found that the phonon component

( $K_{ph}$ ) in the antiferromagnetic state is in agreement with the low-temperature extrapolation of the conductivity values above  $T_N$ . In that region (above  $T_N$ ), the thermal conductivity exhibits a  $T^3$  dependence characteristic of boundary scattering of acoustic phonons at temperatures far below their Debye temperature  $\Theta_D$ . When the phonon mean free path is longer than the smallest crystal dimension, then the mean free path becomes limited by the size of the crystal. The estimated mean free path at 1 K, using a phonon group velocity of  $v_{ph} = 1.5 \times 10^5$  cm/sec and the observed thermal conductivity of  $10^{-2} T^3$  W/cm K, is  $7 \times 10^{-3}$  cm. This is two orders of magnitude less than the smallest dimension of the specimen, which is 0.38 cm. Therefore, the phonon mean free path is not being limited by the geometric boundaries of the specimen but by internal boundaries associated with the mosaic structure of the crystals. Such internal boundaries of various sizes are observed visually.

When the lattice contribution to the thermal conductivity is subtracted from the total conductivity, an excess conductivity ( $K_m$ ) is found which varies with temperature with a  $T^{1.8}$  dependence at temper-

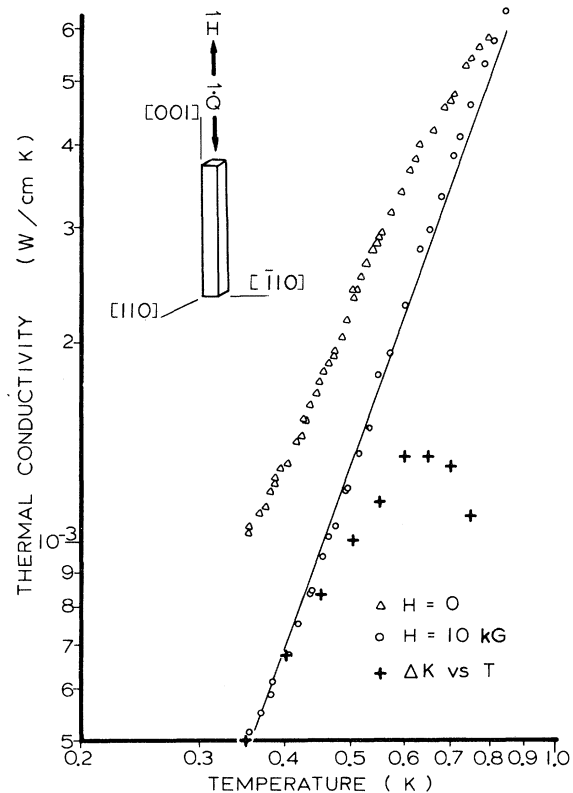


FIG. 9. Thermal conductivity vs temperature on an expanded scale (for  $T < T_N$ ) with magnetic fields of 0 and 10 kG and heat flow in the [001] direction. Also plotted are  $\Delta K = K_0 - K_{10}$  vs  $T$  and a solid line fitting the relation  $K = 1.0 \times 10^{-2} T^3$  W/cm K.

atures less than 0.6 K. This is somewhat suggestive since if the excess conductivity is due to magnons it would, together with the observed magnon contribution to the specific heat, indicate a magnon mean free path which varies as  $T^{-3}$ . If the magnons are primarily scattered by phonons, then one would expect that the magnon mean free path would be inversely proportional to the number of phonons present at a given temperature. However, at low temperatures the number of phonons present is proportional to  $T^3$ . The observed temperature dependence of the proposed magnon contribution is entirely plausible. Furthermore, estimating the magnon group velocity (for  $\vec{q} > 0$ ) from the relation  $v_m = k_B T_N c / \hbar$ , where  $c$  is the lattice spacing in the  $c$  direction, yields a value of  $1.2 \times 10^4$  cm/sec.<sup>20</sup> Incorporating this result with the assumed magnon component of conductivity in zero applied field and the known Debye temperature, one finds a magnon mean free path ( $\sim 10^4$  Å) about two orders of magnitude above that estimated for the average distance between phonons. This result implies a relatively weak magnon-phonon coupling and is consistent with the basic assumption made, namely, that the two possible heat-transport mechanisms are additive in a linear fashion. Strong coupling would vitiate such an analysis.

#### B. Magnetic Phase Diagram

The rather sharp dip in conductivity observed in the region surrounding  $T_N$  for the zero-field curve in Fig. 3 appears to be related to a critical scattering of phonons by fluctuations in the magnon density. Although this phenomenon lacks the sharpness of the temperature dependence observed for specific-heat measurements in zero applied field,<sup>11</sup> it does appear to be a reliable indicator for the paramagnetic-antiferromagnetic phase transition. As an applied field is introduced along the sublattice magnetization direction, this critical scattering dip in a  $K$ -vs- $T$  plot at constant field is seen to shift to lower temperatures. This is an expected result for a typical antiferromagnetic phase diagram. One interesting sidelight to this study is the fact that the depth of the critical scattering dip is strain dependent.

The other phase boundary which can be deduced from the current work is that between the antiferromagnetic and spin-flop regions. A single point on this boundary can be deduced from Fig. 8 in which a reduced conductivity is plotted as a function of field at constant temperature. According to the interpretation placed on these data, the sharp drop in conductivity between 2 and 6 kG occurs as one crosses into the spin-flop region (on going to higher field), and correspondingly the magnon component of the conductivity is destroyed. Similar measurements on another antiferromagnetic

insulator,  $\text{MnCl}_2 \cdot 4\text{H}_2\text{O}$ , by Rives and Walton<sup>21</sup> have shown a similar drop in conductivity which was also interpreted as related to the antiferromagnetic-spin-flop phase boundary. Although Walton's analysis is based solely on phonon transport modified by magnon-phonon interaction, it is noteworthy that either his analysis or the current one is consistent with the notion that a rapid drop in conductivity is indicative of a phase transition.

#### C. Thermal Resonance in Paramagnetic State

The major thrust of the currently reported work has been involved with heat transport in the antiferromagnetic state. Nevertheless, one cannot ignore the striking dependence on applied field and direction of a resonant dip in conductivity observed well within the paramagnetic state. It is possible that this resonant effect involves a spin-phonon interaction, a situation considered theoretically by Orbach.<sup>22</sup>

The resistive resonance may be observed in Figs. 3-6. In Figs. 3 and 6, the applied field is in the [001] direction. Although the direction of heat differs (by a rotation of  $90^\circ$ ) for these two figures, the resonant characteristics are qualitatively similar, e. g., at 10 kG the resistive resonance is spread entirely over the temperature range 2-8 K. Correspondingly, in Figs. 4 and 5, the applied field is in the  $[\bar{1}10]$  and [110] equivalent directions. Similarly, for these two figures, although heat flows in a different (perpendicular) direction for these two sets of curves, the resonant characteristics are qualitatively similar again, e. g., at 10 kG there is a reduction in conductivity starting at the (zero-field) peak-conductivity temperature and extending to lower temperatures below  $T_N$ .

The resonant features of these data are pronounced, especially when they are replotted in terms of a reduced thermal resistivity vs temperature. Huber<sup>23</sup> has treated the problem of spin-lattice coupling which in a paramagnetic material gives rise to a resonance as observed. However, his analysis is based on the assumption that the spin-phonon interaction occurs for a band of phonon frequencies which would otherwise interact resistively only with the crystal boundaries. This is certainly not the case in the present situation where the resonant behavior (for a 10 kG applied field or greater) occurs in the region of the thermal-conductivity maximum. Analyzing the data of Figs. 3-6 on the basis of the qualitative relation  $g\mu_B H \approx k_B T$ , it is found that  $g \sim 11$  along the [001] direction and that  $g \sim 3$  along the  $[\bar{1}10]$  or [110] direction.

The observation of only a single spin-phonon resonance over the experimental range of temperature and magnetic field supports the initial suppo-



sition that only the lowest-lying doublet need be considered. Implicit also in this assumption is the fact that there is a considerable amount of overlap of the  $3d^7$  electrons of Co with the orbitals of the six ligands in a tetragonal structure, forming covalent bonds with these ligands and leaving one electron unpaired.

The significance of the observed resonance behavior is that while thermal conductivity provides none of the precision afforded by electron-spin-resonance (ESR) measurements, it may provide the only data on the anisotropy of  $g$  and the width of the Kramers doublet. This is particularly so when the paramagnetic ion is a constituent part of each unit cell, as saturation effects would obscure the ESR observed for a system of lower concentration. An attempt to observe an ESR absorption in cobalt chloride thiourea was unsuccessful due to saturation.<sup>24</sup>

In the absence of chemical analysis and data from a large body of crystal specimens, the above discussion must be tempered by the possibility that paramagnetic impurities could produce a thermal resonance as observed.

#### V. CONCLUSION

The foregoing results and analysis of thermal-conductivity measurements on cobalt chloride thiourea show that one can interpret the data in the antiferromagnetic state as arising from magnon, as well as phonon, heat transport. The magnitude of the magnon component is qualitatively acceptable. Its temperature dependence is consistent with that of specific-heat data and the assumption that magnon scattering is dominated by phonon interaction at temperatures less than 0.6 K.

The notion that the observed data can be interpreted solely upon the basis of phonon heat transport is implausible. This is so because the thermal conductivity (in the [001] direction) below  $T_N$  shows a distinct *enhancement* over the extrapolated  $T^3$  dependence of the conductivity observed in the paramagnetic state. This is contrary to the behavior observed by Rives and Walton<sup>21</sup> for  $MnCl_2 \cdot 4H_2O$  in which the temperature-dependent data show a *decrease* in conductivity below  $T_N$  with respect to the extrapolated data at higher temperatures. For such behavior, a significant contribution by magnon heat transport is not expected. This is not the case in the current study.

While the interpretation of the data on the basis of magnon transport seems plausible and consistent, there are some questions which remain to be answered. In principle, there is no reason in general why magnon transport cannot occur in a direction normal to the sublattice magnetization. However, it is well known that the system under investigation is magnetically and mechanically anisotropic. The

dispersion relation for magnons and the magnon-phonon coupling should also be anisotropic.

The most disturbing unresolved question concerns the increase in conductivity (in the [001] direction) for fields in excess of 10 kG. Analysis of these data (for a 20-kG field) on the basis of two-component heat transport does yield a consistent value for the phonon component and a  $T^2$  dependence for the other. Assuming this analysis to be valid, one must assume that the intense magnetic field in the spin-flop state produces sufficient parallel spin alignment to support the excitation of ferromagnetic-type magnons. Specific-heat measurements in the spin-flop region will be carried out to test this supposition. However, it is interesting to note that Wang and Callen<sup>25</sup> have shown that long-range excitation is possible in the spin-flop state, although their analysis does not apply in detail to the present study.

#### ACKNOWLEDGMENTS

The authors wish to acknowledge helpful discussions with Professor M. H. Cohen of the University of Chicago and Professor C. K. Chau of the Illinois Institute of Technology.

#### APPENDIX: SOME PHYSICAL PROPERTIES OF COBALT CHLORIDE THIOUREA, $Co[(NH_2)_2CS]_4Cl_2$

The following are some physical properties of cobalt chloride thiourea: (i) dielectric; (ii) grown from aqueous solution; (iii) color, dark blue; (iv) shape, bipyramidal; (v) x-ray analysis; point group,  $4/m$ ; space group,  $P4_2/n$ ; lattice constants, tetragonal  $a = 13.52 \text{ \AA}$ ,  $c = 9.10 \text{ \AA}$ . Assumed unit cell has cobalt ions located at

$$\frac{1}{4} \frac{1}{4} \frac{1}{4}, \frac{1}{4} \frac{3}{4} \frac{3}{4}, \frac{3}{4} \frac{1}{4} \frac{3}{4}, \frac{3}{4} \frac{3}{4} \frac{1}{4};$$

(vi) proton-magnetic-resonance, magnetic-susceptibility, and specific-heat measurements yield the following information: antiferromagnetic alignment with  $T_N = 0.92 \text{ K}$ ; very good approximation to a uniaxial-two-sublattice system; spontaneous magnetization along the [001] direction;  $C_{ph} \propto T^3$ , with  $\Theta_D \approx 65 \text{ K}$ ;

$$S_M (\text{magnetic entropy}) = Nk_B \ln(2S + 1),$$

with  $S = \frac{1}{2}$  for the Co ion;

$$\begin{aligned} H_E (\text{exchange field}) &\approx 6k_B T_N / (S + 1) g \mu_B \\ &= 2.8 \times 10^4 \text{ G} \quad \text{for } g = 2; \end{aligned}$$

$H_A$  (anisotropy field)  $\approx 250 \text{ G}$ , determined from anisotropy in susceptibility and the critical field observed in the current study.

- \*Work supported by the U. S. AEC.  
 †Present address: U. S. Naval Research Laboratory, Washington, D. C. 20390.
- <sup>1</sup>P. W. Anderson, *Phys. Rev.* **86**, 694 (1952).  
<sup>2</sup>I. S. Jacobs, S. Roberts, and P. E. Lawrence, *J. Appl. Phys.* **36**, 1197 (1965).  
<sup>3</sup>S. Foner, S. J. Freiser, and R. W. H. Stevenson, *Phys. Rev. Letters* **9**, 212 (1962).  
<sup>4</sup>F. M. Johnson and A. H. Nethercot, Jr., *Phys. Rev.* **114**, 705 (1959).  
<sup>5</sup>A. Okazaki, K. C. Turberfield, and R. W. H. Stevenson, *Phys. Letters* **8**, 9 (1964).  
<sup>6</sup>H. Sato, *Progr. Theoret. Phys. (Kyoto)* **13**, 119 (1955).  
<sup>7</sup>G. A. Slack, *Phys. Rev.* **122**, 1451 (1961).  
<sup>8</sup>R. H. Donaldson and D. T. Edmonds, *Phys. Letters* **2**, 130 (1962).  
<sup>9</sup>C. J. Gorter and T. van Peski Tinbergen, *Physica* **22**, 278 (1956); C. J. Gorter, *Nuovo Cimento* **6**, 5923 (1957).  
<sup>10</sup>H. Weinstock, *Phys. Letters* **26A**, 117 (1968).  
<sup>11</sup>H. Forstat, N. D. Love, J. McElearney, and H. Weinstock, *Phys. Rev.* **145**, 406 (1966).  
<sup>12</sup>R. Au, J. A. Cowen, and H. Van Till, *Low Temperature Physics-LT9*, edited by J. G. Daunt *et al.* (Plenum, New York, 1965), p. 877.
- <sup>13</sup>D. H. Martin, *Magnetism in Solids* (MIT Press, Cambridge, Mass., 1967), p. 406.  
<sup>14</sup>A. I. Akhiezer, V. G. Bar'yakhtar, and S. V. Peletminskii, *Spin Waves* (North-Holland, Amsterdam, 1968), p. 68.  
<sup>15</sup>F. Keffer, in *Encyclopedia of Physics* (Springer-Verlag, Berlin, 1966), Vol. XVIII, p. 1.  
<sup>16</sup>F. Keffer and C. Kittel, *Phys. Rev.* **85**, 329 (1952).  
<sup>17</sup>Values to obtain this result are  $\chi_{11}/\chi_{12} = 0.23$ ,  $H_C = 4$  kG, and  $g = 2$ .  
<sup>18</sup>R. A. Guenther and H. Weinstock, *J. Appl. Phys.* **42**, 3790 (1971).  
<sup>19</sup>V. Jaccarino, in *Magnetism*, edited by G. T. Rado and H. Suhl (Academic, New York, 1963), Vol. IIA, p. 307.  
<sup>20</sup>The relation  $v_m \approx k_B T_N c / \hbar$  is valid only for systems for which  $H_A \ll H_E$ . The Appendix shows that this condition is satisfied.  
<sup>21</sup>J. E. Rives and D. Walton, *Phys. Letters* **27A**, 609 (1968).  
<sup>22</sup>R. Orbach, *Phys. Letters* **3**, 269 (1963).  
<sup>23</sup>D. L. Huber, *Phys. Letters* **20**, 230 (1966).  
<sup>24</sup>J. Witters (private communication).  
<sup>25</sup>Y. Wang and H. B. Callen, *J. Phys. Chem. Solids* **25**, 1459 (1964).

## Critical Dynamics of the Order-Disorder Transformation in Ferroelectrics\*

D. L. Huber

*Physics Department, University of Wisconsin, Madison, Wisconsin 53706*

(Received 29 June 1972)

The dynamic wave-vector-dependent susceptibility of a model order-disorder ferroelectric is studied with particular emphasis on the contributions from the nonlinear terms in the kinetic equation for the fluctuations in the polarization. The Hamiltonian is that of a spin- $\frac{1}{2}$  Ising model in a weak rapidly fluctuating transverse field which simulates the role played by the phonons in bringing about the reorientation of the dipoles. Nonlinear effects are shown to remain small as  $T$  approaches  $T_c^+$ . As a consequence the susceptibility is quite adequately approximated by the Debye form with a width inversely proportional to the static susceptibility. Below the Curie point the nonlinear terms become much more important. The dominant nonlinear process involves the decay into two fluctuations, a process forbidden by symmetry in the disordered state. The results of the theory are compared with experiment. Agreement is found in some cases. Lack of agreement in others is attributed to the shortcomings of the model.

### I. INTRODUCTION

In recent years interest has grown in the dynamical properties of systems undergoing second-order phase transitions.<sup>1</sup> Among these are, for example, the magnetic transitions (ferromagnetism and antiferromagnetism), the liquid-gas transition near the critical point, the  $\lambda$  transition in liquid helium, various soft-mode structural transitions, and the displacive and order-disorder transitions in ferroelectrics and antiferroelectrics. In analyzing the dynamics particular attention has been paid to the wave-vector-dependent dynamic

susceptibility  $\chi(\vec{q}, \omega)$  which is associated with the order parameter for the transition. In many cases detailed information about the susceptibility has come from inelastic neutron scattering studies where the scattering cross section for momentum transfer  $\hbar\vec{q}$  and energy transfer  $\hbar\omega$  is simply related to  $\chi(\vec{q}, \omega)$ . Although neutron scattering is a versatile probe, it suffers from the limitation that the measurements are hampered by finite resolution. As a consequence phenomena associated with small  $\vec{q}$  and  $\omega$  are sometimes obscured. This is particularly important near the critical point where there frequently is a "softening" of the character-